The crude carbamate was taken up in 5.0 mL of dichloromethane and stirred with 1.0 mL of trifluoroacetic acid for 3 h. The mixture was made basic to pH 11 with aqueous NaOH, the layers were separated, and the aqueous layer was extracted with five 10-mL portions of dichloromethane. Drying and concentration gave 0.076 g (78%) of the free base **12**: ^{1}H NMR ($CDCl_3$) δ 6.81 (1 H, br s, N*H*), 2.97 (1 H, m, C-8a *H*), 2.62 (1 H, br m, C-2 *H*); HRMS, calcd for $C_{13}H_{25}N$ 195.1987, found 195.197.

The **hydrochloride** was prepared and recrystallized from a mixture of isopropyl alcohol and ether (3:1 v/v), mp 231-233 °C (lit.[12a] mp 243-244 °C): IR (KBr) 3400, 2530, 1585, 1480, 1467, 1438, 1390, 1195, 1130, 982, and 960 cm^{-1}; ^{1}H NMR ($CDCl_3$) δ 3.32 (1 H, m), 2.96 (1 H, br m), 0.96 (3 H, t, J = 6.0 Hz), 0.88 (3 H, d, J = 6.2 Hz); ^{13}C NMR ($CDCl_3$-D_2O) 60.1, 58.0, 41.0, 35.0, 34.6, 29.2, 27.4, 25.3, 23.2, 20.7, 19.8, 18.8, and 13.8 ppm (lit.[12a] ^{13}C NMR 60.1, 58.1, 41.0, 35.0, 34.6, 29.2, 27.4, 25.3, 23.3, 20.7, 19.8, 19.2, and 13.7 ppm).

Acknowledgment is made to the donors of the Petroleum Research Fund, administered by the American Chemical Society, for support of this work.

Crystal Structure of the Covalent Complex Formed by a Peptidyl α,α-Difluoro-β-keto Amide with Porcine Pancreatic Elastase at 1.78-Å Resolution†

Lori H. Takahashi,‡ R. Radhakrishnan,§ Richard E. Rosenfield, Jr.,§ Edgar F. Meyer, Jr.,*,§ and Diane Amy Trainor‖

Contribution from the Department of Chemistry, Texas A&M University, College Station, Texas 77843, Department of Biochemistry and Biophysics, Texas A&M University, College Station, Texas 77843-2128, and Stuart Pharmaceuticals, Division of ICI Americas Inc., Wilmington, Delaware 19897. *Received October 12, 1987. Revised Manuscript Received October 13, 1988*

Abstract: The crystal structure analysis of the covalent enzyme–inhibitor complex of porcine pancreatic elastase (PPE) with a peptidyl α,α-difluoro-β-keto amide has shown that the tightly bound inhibitor forms an hemiketal complex with the O$^\gamma$ atom of the catalytic Ser-195 and is stabilized by five intermolecular H bonds and optimal van der Waals' surface interactions. The inhibitor is bound to the enzyme in an antiparallel β-pleated sheet arrangement. The carbonyl oxygen atom of the inhibitor is situated in the "oxyanion hole", hydrogen bonded to the amido nitrogen atoms of Ser-195 and Gly-193. A strong hydrogen bond between His-57 and a fluorine atom also aids in stabilizing the complex. The H-bonding catalytic tetrad of elastase is structurally intact. Covalent attachment of ligand plus active site Ser-195 is based upon contiguous electron density found in the initial, unbiased difference Fourier electron density map. The resulting hemiketal linkage has chemical and structural similarities with the putative tetrahedral intermediate of a productive enzyme–peptide ligand complex. This analysis provides structural evidence for the preferred binding of a novel class of inhibitors of the serine proteinases. Two refinement programs, EREF and TNT, were used to refine the enzyme + inhibitor model.

Elastases (EC 3.4.21.11) are possibly the most destructive enzymes in the body, having the ability to degrade virtually all connective tissue components. Elastases are involved in the pathogenesis of pancreatitis and emphysema.[1,2] They have also been implicated in atheroschlerosis,[3] adult respiratory distress syndrome,[4] rheumatic arthritis,[5] and other disease states.[6]

Peptidyl fluorinated ketones have been shown to be excellent inhibitors of the elastases. Imperiali and Abeles,[7] Kolb,[8] and Trainor[9] have synthesized potent peptidyl difluoromethylene ketone and peptidyl trifluoromethyl ketone inhibitors of HLE[10] and PPE. Kinetic analysis of some of these fluorinated ketones suggests that these compounds are transition-state analogue inhibitors.[7,11,12] The enhanced electrophilicity of the fluorinated ketone carbonyl was expected to facilitate an enzyme-catalyzed addition of the active site serine to the ketone carbonyl, forming a stable hemiketal intermediate.

To establish unequivocally the nature of the complexation of PPE with a peptidyl α,α-difluoro-β-keto amide, (*S*)-*N*-acetyl-L-alanyl-*N*-[3,3-difluoro-1-(1-methylethyl)-2,4-dioxo-4-[(2-phenylethyl)amino]butyl]-L-prolinamide (**1**) was prepared for crystallographic analysis. Additional interactions between the S′ subsites (nomenclature of Schechter and Berger[13]) of the enzyme and the P′ fragments of the peptidyl difluoro ketone inhibitors

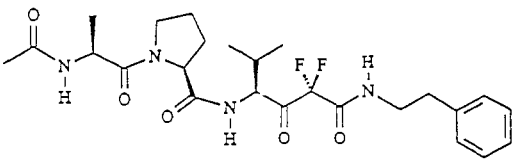

1

were believed to contribute to the overall tight binding. Subsequent analogues could then be designed for more specific S′–P′ inter-

†This work was supported in part by the Office of Naval Research (Grant K0662), The Robert A. Welch Foundation (Grant A328), and by The Council for Tobacco Research, U.S.A. (Grant 1849).

‡Dept. of Chemistry, Texas A&M University.
§Dept. of Biochemistry and Biophysics, Texas A&M University.
‖Stuart Pharmaceuticals.

(1) Geokas, M. C.; Rinderknecht, H.; Swanson, V.; Haverback, B. J. *Lab Invest.* **1986**, *19*, 235-239.
(2) Mittman, C. *Pulmonary Emphysema and Proteolysis* Academic Press: New York, 1971; pp 1-537.
(3) Janoff, A. *Annu. Rev. Med.* **1985**, *36*, 207-216.
(4) Burchardi, H.; Stokke, T.; Hensel, T.; Koestering, H.; Ruhlof, G.; Schlag, G.; Heine, H.; Horl, W. H. *Adv. Exp. Med. Biol.* **1984**, *167*, 319-333.
(5) Janoff, A. In *Neutral Proteinases in Human Polymorphonuclear Leukocytes*; Havemann, K., Janoff, A., Eds.; Urban and Schwartzenberg: Baltimore, MD, 1987; pp 390-417.
(6) Stein, R. L.; Trainor, D. A.; Wildonger, R. A. *Annu. Rep. Med. Chem.* **1985**, *20*, 237-246.
(7) Imperiali, B.; Abeles, R. H. *Biochemistry* **1986**, *25*, 3760-3767.
(8) Kolb, M.; Barth, J.; Neises, B. *Tetrahedron Lett.* **1986**, *27*, 1579-1582.
(9) Trainor, D. A. Tenth American Peptide Symposium (Abstracts), Washington University, St. Louis, MO, 1987.
(10) Abbreviations: MEO, methoxy; SUC, succinyl; PNA, *p*-nitroaniline; DFK, difluoro ketone; PPE, porcine pancreatic elastase; HLE, human leucocyte elastase; Vaf, a valine residue with a difluoromethyl hemiketal group in place of the carbonyl group ($COCF_2$); Pea, β-ketophenethylamide; rms, root-mean-square; BPTI, bovine pancreatic trypsin inhibitor.

0002-7863/89/1511-3368$01.50/0

actions, leading to enhanced specificity. Receptor subsites for PPE are listed in Table II of ref 14. We previously studied[15] the complex of PPE with a peptidyl trifluoromethyl ketone. The structure reported here thus adds information about the structural role of fluoro ketones and especially interactions in the S′ region of the extended binding site. The bulk of the chemical and structural literature on PPE refers to inhibitors or ligands lacking S′ functionality; thus, much less is known about receptor:ligand interactions on the P′ "leaving group" side. Kinetic analysis of **1** has shown that it is a potent ($K_i = 1 \times 10^{-7}$ M at pH 7.8 and 5.4×10^{-6} M at pH 5.5) competitive inhibitor of PPE when analyzed versus the synthetic substrate MEO-SUC-Ala-Ala-Pro-Val-PNA, using a reported[12] analytic method. The K_i[15] at pH 5.5 of the analogous peptidyl trifluoromethyl ketone, 9.5×10^{-6} M, is only slightly greater than that of this compound, indicating enhanced interactions gained in the S′ region with the difluoro ketones versus partial loss of electronegativity as a result of functional replacement of the third F atom.

Mechanistically, PPE exhibits "fast" binding with **1** at pH 5.5, while HLE exhibits slow binding.[16] More structural information, especially from HLE complexes, will be required before this structure–function relationship can be clearly defined.

Refinement

Crystallographic refinement was performed as previously described[14] with the PROTEIN[17] system of programs together with reciprocal space refinement with energy restraints using program EREF[18,19] modified and implemented by Deisenhofer.[20] The initial difference Fourier map was calculated by using phases and amplitudes from the coordinates of the 1.65-Å resolution native enzyme structure[14] with active site solvent molecules and ions removed. The unbiased electron density for the inhibitor was continuous with the electron density of the enzyme at Ser-195 O^{γ}, indicating a covalent adduct. Inactivation of the enzyme by the inhibitor results in the formation of a hemiketal covalent bond (1.47 Å) between the inhibitor Vaf[10] carbonyl carbon atom (*R* - configuration) and the active site Ser-195. Unambiguous density was found in the P_2–P_1' region; density at the two termini was more diffuse prior to refinement.

Initial coordinates for the inhibitor molecule were generated with standard bond lengths, bond angles, and dihedral angles, using program FRODO.[21] The model was fit into the residual electron density and added after the initial cycles of refinement. Individual temperature factor shifts were calculated for each atom from the difference Fourier synthesis with program DERIV and were applied after each refinement series. For the Fourier synthesis calculation, reflections with poor correlation were excluded by the use of a rejection ratio, defined as

$$(2||F_{obsd}| - |F_{calcd}||)/(|F_{obsd}| + |F_{calcd}|) > 1.2$$

Peaks were identified as water molecules when they had a well-defined electron density (ca. 0.25 e/Å^3) and were within an acceptable distance from at least one other polar protein group or another water molecule. Target refinement geometries and constraints not provided in the EREF library, derived from values given by Levitt,[19] are given in Table I, which also contains final values of these specific distances and angles.

Table I. Optimum Values and Refined Values for Some of the Parameters

param	optimum	refined	wt given
OG–C	1.46 Å	1.48 Å	400.0
F–C	1.34 Å	1.28 Å	384.0
O–C–O	110.7°	106.5°	60.0
C–O–C	112.1°	116.9°	60.0
O–C–C	109.5°	120.8°	50.0
F1–C1–C	109.7°	112.6°	55.0
F2–C1–C	109.7°	119.5°	55.0
F1–C1–F2	107.0°	97.5°	47.0

Table II. Final Parameters for the Complex

R factor ($=\sum||F_o| - |F_c||/\sum|F_o|$)	0.16
resolutn range, Å	7–1.78
effective resolutn,[23] Å	1.98
no. of reflcns	16 151
no. of atoms	2005
overall temp factor for complex, Å^2	13.4
overall temp factor for inhibitor, Å^2	20.9
SD for bond length, Å	0.012
SD for bond angle, deg	2.28
min and max cutoff for temp factor, Å^2	4.0 and 45.0
min and max electron density in final ΔF map, e/Å^3	−0.35 and 0.36
mean positnal error,[24] Å	0.2

A total of 70 refinement cycles of both positional and isotropic thermal parameters was calculated and 142 water molecules were located.

As refinement proceeded, an unusual geometric interaction developed about the carbonyl–hemiketal C atom: the Ser-195 O^{γ}–C–C_1 bond angle appeared to be almost trigonal, 120°. However, the initial, unbaised difference Fourier map clearly showed contiguous electron density indicative of covalent attachment, an hemiketal. Yet, when the crystallographic contribution (i.e., difference Fourier map) was given more weight than idealized geometric restraints, the angle about the central C atom increased toward 120°.

We therefore initiated independent refinement using program TNT,[22] with restraints based upon geometry rather than "pseudoenergy". Geometric restrains for standard amino acids are contained within program TNT. Values pertinent to this complex were averaged from the small-molecule crystallographic literature and include the following: C–F (1.34 Å), C–O^{γ} (1.46 Å), C–OH and C–O^- (1.37 Å), F–C–F (107.0°), C–X–C (113.3°, X = CF_2 group). The pertinent angle (O^{γ}–C–C_1F_2) decreased to 113.6° but at the expense of the next chain backbone angle, C–C_1F_2–C_2, which increased from 114.6 to 116.5°. The standard deviations of standard bond lengths and angles changed slightly (from 0.012 to 0.014 Å and 2.32 to 2.23°); the *R* factor increased from 0.16 (EREF) to 0.18 (TNT). This latter value is not readily comparable because no rejection ratio is employed in TNT, but a solvent contribution function is employed. As this angular discrepancy is just at the 3σ level, we are not able to attach more structural significance to it, beyond the reflection that refinement contributions along both ends of the inhibitor chain appear to be focused at this point, producing a moderate flattening effect that is neither program nor refinement parameter dependent. Flexibility is also reduced in this region by steric constraints at both hemiacetal O atoms as well as to the one F atom.

Due to the similarity of results, the structural model obtained from EREF refinement will be used for subsequent discussion. The final refinement parameters for the enzyme–inhibitor complex are summarized in Table II. Occupancy was not refined; inhibitor temperature factors ranged from 18.6 to 24.6 Å^2, indicative of ordered binding; greater flexibility is exhibited by terminal atoms,

(11) Gelb, M. H.; Svaren, J. P.; Abeles, R. H. *Biochemistry* **1985**, *24*, 1813–1817.
(12) Stein, R. L.; Strimpler, A. M.; Edwards, P. D.; Lewis, J. J.; Mauger, R. C.; Schwartz, J. A.; Stein, M. M.; Trainor, D. A.; Wildonger, R. A.; Zottola, M. A. *Biochemistry* **1987**, *26*, 2682–2689.
(13) Schechter, I.; Berger, A. *Biochem. Biophys. Res. Commun.* **1967**, *27*, 157–162.
(14) Meyer, E.; Cole, G.; Radhakrishnan, R.; Epp, O. *Acta Crystallogr.* **1988**, *B44*, 26–38.
(15) Takahashi, L. H.; Radhakrishnan, R.; Rosenfield, R. E.; Meyer, E. F.; Trainor, D. A.; Stein, M. *J. Mol. Biol.* **1988**, *201*, 423–428.
(16) Stein, R. L.; Strimpler, A. M. *J. Am. Chem. Soc.* **1987**, *109*, 6533–6540.
(17) Steigemann, W. Ph.D. Thesis, T.U. Munchen, 1974.
(18) Jack, A.; Levitt, M. *Acta Crystallogr.* **1978**, *34A*, 931–935.
(19) Levitt, M. *J. Mol. Biol.* **1974**, *82*, 393–420.
(20) Deisenhofer, J.; Remington, S. J. Steigmann, W. *Methods Enzymol.* **1985**, *115B*, 303–323.
(21) Jones, T. A. *J. Appl. Crystallogr.* **1978**, *11*, 268–272.
(22) Tronrud, D. E.; Lynn, F.; Ten Eyck, L. F.; Matthews, B. W. *Acta Crystallogr.* **1987**, *A43*, 489–501.
(23) Swanson, S. M. *Acta Crystallogr.* **1988**, *A44*, 437–442.
(24) Luzatti, V. *Acta Crystallogr.* **1952**, *5*, 802–810.

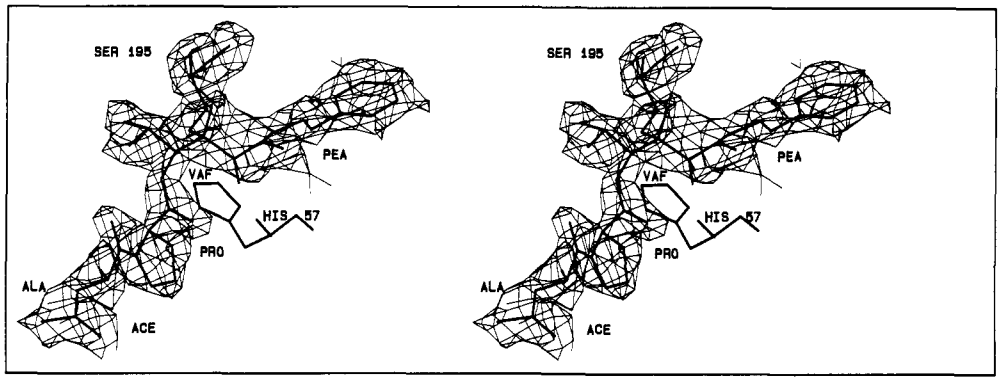

Figure 1. Final difference Fourier ($F_o - F_c$) map with the final model of the inhibitor superimposed. The contouring level is 0.14 e/Å^3. The covalently bonded difluoromethyl hemiketal valine moiety is labeled Vaf here and in Figure 2.

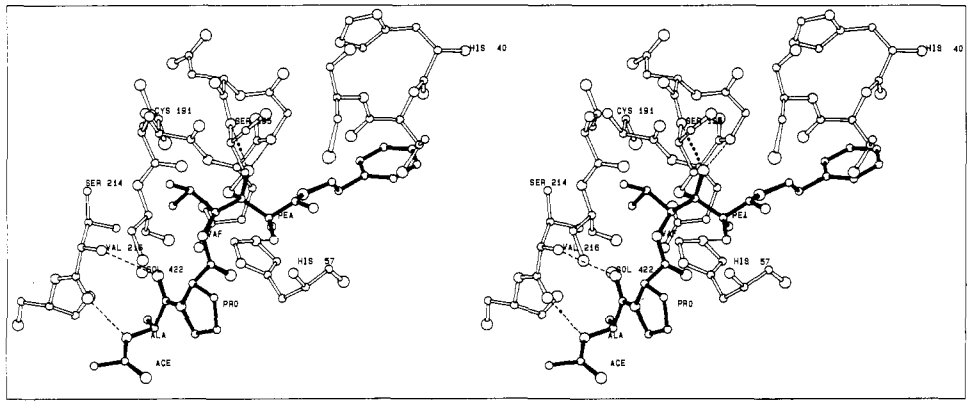

Figure 2. Stereoview of the inhibitor in the extended binding site of PPE. Hydrogen bonds are represented by dashed lines.

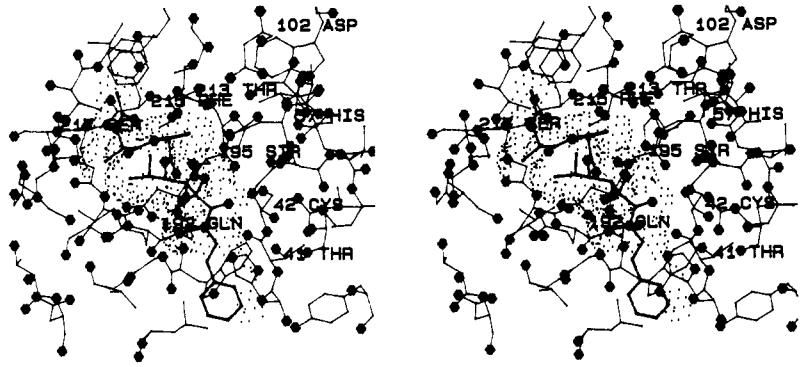

Figure 3. Stereoview of the extended binding site of PPE (thin lines) containing the peptidyl fluoromethyl ketone inhibitor (heavy line). N and O atoms are indicated by "spots" created by routine BLOB (A. Karrer, unpublished), which has been submitted for inclusion in program FRODO.[21] The extent of receptor–ligand interaction is illustrated by the 2.0 vs 2.0 Å contact surface, generated by the INTER function of program FRODO.

as is found in similar complexes.[15,25]

Results and Discussion

The difference electron density map using data to 1.78 Å resolution is illustrated in Figure 1. In the same orientation, Figure 2 illustrates the location of the inhibitor in the extended binding site of PPE.

The receptor site of PPE has been described by Thompson and Blout[26] and incorrectly by Atlas[27] and consists of at least eight subsites (cf. Table II, ref 14). The primary specificity pocket of PPE (S1) is hydrophobic,[28] consisting of the residues of Thr-213 to Val-216, Thr-226, and Val-227, which explains the enzyme's preference for hydrophobic, nonpolar, unbranched amino acids. The occlusion of the binding pocket by the side chains of Val-216 and Thr-226, which replace the corresponding Gly residues of trypsin and chymotrypsin, narrows the specificity of the S1 subsite to amino acids with small aliphatic side chains. The P1 Val (Vaf[10])

Table III. Hydrogen Bonds in the Active Site of the Complex

inhibitor	enzyme	donor–acceptor dist, Å	angle at H, deg
	Intermolecular Hydrogen Bonds		
Ala > NH	O=C < Val-216	2.64	152
Ala > C=O	HN < Val-216	2.91	155
Val > C=O	HN < Ser-195	2.97	135
Val > C=O	HN < Gly-193	2.58	139
Vaf > C-F	$HN^{\epsilon 2}$ < His-57	2.76	144
	Intramolecular Hydrogen Bonds		
Ser-195 > O^{γ}	$HN^{\epsilon 2}$ < His-57	3.03	112
Asp-102 > $O^{\delta 2}$	$HN^{\delta 1}$ < His-57	2.60	173
Ser-214 < O^{γ}	$O^{\delta 1}$ < Asp-102	2.71	170
Gln-192 > $O^{\epsilon 1}$	HN < Glu-192	2.84	138
Gly-193 > O	$HN^{\epsilon 2}$ < His-40	2.96	152
Cys-191 > O	HN < Asp-194	2.92	160

(25) Meyer, E.; Clore, G. M.; Gronenborn, A. M.; Hansen, H. A. S. *Biochemistry* **1988**, *27*, 725–730.
(26) Thompson, R. C.; Blout, E. F. *Proc. Natl. Acad. Sci. U.S.A.* **1970**, *67*, 1734–1740.
(27) Atlas, D. *J. Mol. Biol.* **1975**, *93*, 39–53.
(28) For enumeration of PPE receptor subsites: cf. Table II, ref 14.

residue of the inhibitor is located in the primary specificity site (S1) and is involved in van der Waals' interactions with the S1 hydrophobic side chains as shown in Figure 3.

For the analysis of hydrogen bond lengths and angles, the coordinates of the hydrogen atoms were generated from the final set of atomic coordinates with the program HYDGEN (Radhakrishnan, R., unpublished results). Hydrogen atoms were added onto donor atoms in geometrically feasible positions taking into account both the covalent and hydrogen-bonding stereochemistry.

The carbonyl O atom of the Vaf residue is within hydrogen-bonding distance of the backbone amide N atoms of Gly-193 and Ser-195, which form the "oxyanion hole"[29] (see Table III). The tetrahedral intermediate is stabilized by these two hydrogen bonds from the enzyme to the carbonyl O atom of the substrate. It is difficult to predict from available crystallographic studies if these H bonds are formed earlier in the Michaelis complex or only later in the tetrahedral intermediate. The structure of pancreatic trypsin inhibitor noncovalently bound to bovine trypsin[30] demonstrated good H bonding in the oxyanion hole upon binding and suggests tetrahedral distortion about the C atom of the scissile peptide bond. The Michaelis complex formed by PPE and an N-methylated hexapeptide[25] suggests that the oxygen atom fits initially in the oxyanion hole but that a neighboring water molecule (408) competes with Ser-195 >NH for ideal placement of the carbonyl O atom.

This complex exhibits the same antiparallel β-pleated sheet bonding arrangement as in the structure of trypsin with BPTI[30] and HLE[31]. (The homology of the active sites of PPE and HLE is illustrated in Figure 4 of ref 32 and in a recent review.[33]) However, there is no H bond between the Vaf amido N atom and Ser-214, in common with other oligopeptide complexes of this series. There is also no H bond between the inhibitor Pro carbonyl O atom and Glu-192 N^{ϵ}, the distance being 4.17 Å. Similarly, no S2-P2 H bonds are found for the *Streptomyces griseus* or chymotrypsin complexes with peptidic aldehydes;[34] a carbonyl O atom–Gln 192 NE2 H bond (3.1 Å) is found in the trypsin–leupeptin complex.[35] While Delbaere and Brayer[34] report a tight van der Waals' fit for the P2 Leu of the synthetic peptide aldehyde, which causes the entire inhibitor to be shifted by 0.9 Å: here, because P1 Pro faces away from the receptor and out into solution, no strong repulsions and shifts occur at this site.

The amido N atom of the Ala residue in P3 forms an antiparallel β-sheet arrangement by hydrogen bonding to the Val-216 carbonyl O atom; also the carbonyl O atom of Ala forms an H bond with the amido N atom of Val-216. Thus, the hydrogen bonds in the β-sheet arrangement here involve only P3 Ala and P1 Vaf.

There are five intermolecular H bonds between the inhibitor and the enzyme; the H bonds in the active size of the complex are summarized in Table III. This may be compared to the six H bonds found in the trypsin–BPTI complex.[30] As in the analogous trifluoromethyl ketone complex,[15] an additional 2.76 Å contact distance (presumably a N–H···F H bond) between His-57 and one of the F atoms of the inhibitor is found.[36] This bond is considerably shorter (i.e., stronger) than the comparable H bond in the PPE complex of the peptidyl trifluoromethyl ketone (3.1 Å). Figure 2 shows the final model of the inhibitor in the active site of PPE.

Gly-193 NH is involved in an H bond to one of the sulfate O atoms in the native PPE structure,[14] but the bond is not found here because the sulfate ion has been displaced by the fluorinated C atom of Vaf in the S1′ site; Gly-193 is also involved in the H-bonding pattern of the oxyanion hole. Also, one of the O atoms of the sulfate ion in the native structure makes a weak H bond with His-57 N^{ϵ}, which here makes a strong H bond with a F atom of the inhibitor.

The phenylethyl group of Pea is too long to fit into the S1′ pocket and therefore is displaced into the S2′ subsite. Thermal motion in this region (B = 21.6 Å^2) is higher than that of the Vaf group (B = 19.9 Å^2), suggesting more positional freedom, corresponding to the absence of H-bonding and strong interactions. Partial occupancy may be excluded on the basis of tight binding (K_i = 5.4 μM), fast reaction kinetics, and an excess of substrate in the mother liquor. While van der Waals' interactions predominate here in the S′ region, this analysis indicates the value of the subsequent design of P′ functional groups chosen to be complimentary to specific S′ interactions.

The accessibility of the van der Waals' surface of the free and bound inhibitor atoms was calculated to be 240 and 50 Å^2, respectively, using the program ACCESS[37] with a probe sphere of radius 1.4 Å. Of the total accessibility calculated for the bound inhibitor, ca. 50% is contributed by the benzene ring of the Pea group, which may be an indication that the Pea terminal group is not uniquely bound. This suggests in a more quantitative way that functional groups in the P′ region may be more appropriately chosen to improve specific binding interactions with S′ subsites. Such modifications have been proposed from our modeling studies; second generation compounds have been synthesized and will soon be subjected to crystallographic analysis.

The disordering of solvent accompanying inhibitor binding may be held to provide a favorable entropic contribution to the free energy of binding for the inhibitor. Three water molecules found in the native PPE structure[14] were displaced from the active site as a consequence of inhibitor binding. Sol-415 is displaced by the inhibitor Pro residue in the P2 subsite. Another water molecule (Sol-514) is located at the entrance to the S1 site and is displaced by the Vaf residue in the primary specificity pocket. The Pea group displaces one other water molecule (Sol-513) in the S1′–S2′ region. However, the water cluster consisting of Sol-319-320-321 is structurally conserved in the active site region and may play an essential role in the catalysis of larger substrates.[14] Sol-320 makes an H bond with the amido N atom of Asp-102 (3.14 Å here, 3.0 Å native). The catalytic tetrad is completely shielded from bulk water by the bound ligand.

(29) Henderson, R. *J. Mol. Biol.* **1970**, *54*, 341–354.

(30) Huber, R.; Bode, W.; Kukla, D.; Kohl, U.; Ryan, C. A. *Biophys. Struct. Mech.* **1975**, *1*, 189–201.

(31) Bode, W.; Wei, A.-Z.; Huber, R.; Meyer, E.; Travis, J.; Neumann, S. *EMBO J.* **1986**, *10*, 2453–2458.

(32) Meyer, E. F.; Bode, W. The Study and Design of Specific Inhibitors to Elastase. In *QSAR in* Drug *Design and Toxicology*; Hadzi, D., Jerman-Blazic, B., Eds.; Elsevier: Amsterdam, The Netherlands, 1987; pp 247–254.

(33) Meyer, E. *Molecular Modelling*, Xth International Symposium on Medicinal Chemistry, Budapest; Pallos, L., Timmerman, H., Eds.; Elsevier Science: Amsterdam, The Netherlands, in press.

(34) Delbaere, L. T. J.; Brayer, J. T. *J. Mol. Biol.* **1985**, *183*, 89–103.

(35) Walter, J.; Radhakrishnan, R.; Meyer, E. F.; Bode, W., Manuscript in preparation.

(36) As X-ray methods at this resolution are unable to establish the presence (or absence) of individual H atoms, the N–H···F bond can only be postulated between His-57 N^{ϵ} and Vaf. However, the K_i at pH 7.8 is 54 times lower (1×10^{-7} M) than the K_i at pH 5.5 (5.4×10^{-6} M), suggesting no serious loss of this interaction, this being the only proximal functional group with a pK_a near physiological pH (ca. 6.5). While an alternative binding mode cannot be excluded without a crystallographic determination at pH 7.8, the study of binding of a tripeptide, Ac-Ala-Pro-Ala, to PPE at pH 5.0[36] and at pH 7.5 (manuscript in preparation) shows no substantive differences in binding preferences. Likewise, because this analysis was undertaken at pH 5.0, below the normal pK_i for His (6.5), both imidozole N atoms are presumably protonated. The time-averaged structure represented by the refined structure suggests a dual H-bonding interaction. A "pseudo bond angle" may be calculated by placing a "pseudo atom" midway along the C^{γ}–N^{δ} bond; thus, a bond angle X–N–Y should ideally be 180° for an optimal H bond. The angle to O^{γ} of Ser-195 is 120° with a distance of 3.0 Å; this is indicative of a very weak interaction. The angle to the F atom is 143° and the distance is 2.43 Å; this comes much closer to being an acceptable H bond. Because of the bound inhibitor, the charge-relay system need no longer function for the product complex. The resulting structure may therefore represent the average of two competing H-bonding geometries. At physiological pH, it is rather a matter of speculation what the protonation state of the buried His-57 NE2 atom might be; both the unprotonated state (lone-pair elements; OH···N<) and protonated state (>N–H···F) offer opportunities for a structured H bond.

(37) Lee, B.; Richards, F. M. *J. Mol. Biol.* **1971**, *55*, 379–400.

Scheme I[a]

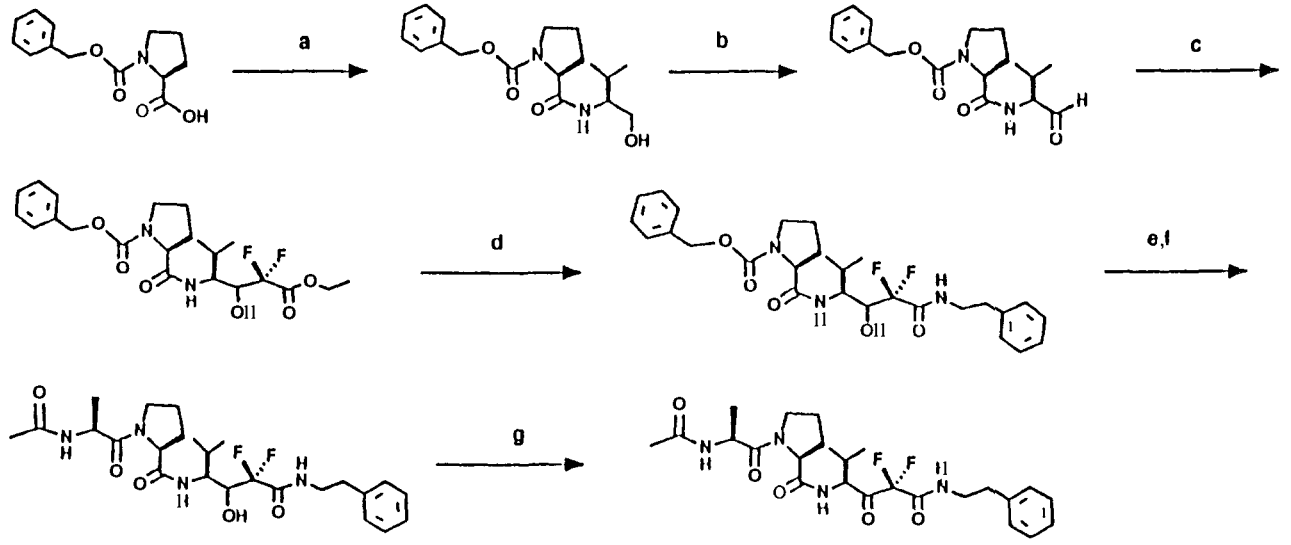

[a](a) L-Valinol, *I*-BuOCOCl, NMM, THF, -20 °C; (b) $(COCl)_2$, DMSO, CH_2Cl_2; (c) $BrCF_2COOEt$, Zn, THF, reflux; (d) $PhCH_2CH_2NH_2$, EtOH, reflux; (e) 10% Pd/C, H_2, EtOH; (f) Ac-L-Ala, WSCDI, HOBt, CH_2Cl_2; (g) Dess-Martin periodinane, TFA, CH_2Cl_2.

A slight repositioning and increase in the apparent Debye–Waller temperature factors has occurred for the Asp-102 residue (8.3 vs 5.8 Å^2 in the native[14] structure) as a consequence of inhibitor binding. The repositioning here involves a 7.0° rotation about the C^β–C^γ axis, which can aid in giving a more linear H bond between the side chains of the amido N atom of Gly-193 and the Vaf O atom in the oxyanion hole. This also leads to a more favorable H bond length (2.7 Å) between Asp-102 $O^{\delta 1}$ and Ser-214 O^γ. The hydrogen bond angle changes by 6.0°. The His-57 N^δ–Asp-102 $O^{\delta 2}$ H bond has not changed (2.59 Å in both). The Ser-195 X^1 angle (C^β–C^α–N-Asp-194) in the complex is 169.4°, whereas in the native structure it is 163.4°. The Ser-195 X^2 angle (O^γ–C^β–C^α–N) is 105.5° in the native structure and 108.4° in the complex. The rest of the protein is relatively unperturbed as a consequence of inhibitor binding. Comparison with the native 1.65-Å PPE structure[14] yielded a rms deviation of 0.16 Å for 817 of 860 backbone atoms.

The structure of the homologous trifluoromethyl ketone–PPE complex has been determined to 2.57-Å resolution.[15] The backbone atoms (NCCO) of these two ligands may be superimposed with a rms agreement of 0.26 Å; likewise, the Ala-Pro-Val (NCCO) skeleton reported here agrees to rms 0.50 Å with the chloromethyl ketone complex of HLE.[38] Although PPE and HLE have a sequential homology of only 41%,[33] 528 backbone atoms common to HLE[31] and this structure agree to rms of 0.48 Å. The agreement is even more striking when the central receptor residues (57, 102, 189–195, 213–216, 226, 228) are superimposed: 55 backbone (NCCO) atoms agree to a rms fit of 0.26 Å, the greatest divergence occurring at amino acids 192 and 226.

Conclusion

In order to explore the mode of binding of this novel class of inhibitors, a compound (**1**) was especially synthesized and then allowed to react within a large, single crystal of PPE. The high-resolution crystallographic data were refined by a crystallographic plus energy method (EREF) and independently with a crystallographic plus geometric method (TNT), and an unambiguous model of the complex was obtained. This result now points the way to the design of inhibitors with specific interactions in the S′ region of the receptor.

The collaboration of chemistry and crystallography thus established the binding geometry of this complex, adding to the data base of small-molecule ligands bound to the serine proteases. Such information is of crucial importance for a rational approach to drug design by means of molecular modeling. Whereas in trypsin or kallikrein, P_1–S_1 Coulombic forces play a dominant role in fixing the ligand to the S_1 receptor pocket, elastase and related enzymes bind an extended peptide substrate with only a few H bonds, which, together with the interactions of assorted backbone dipoles and collective van der Waals' forces, determine specificity and catalytic complimentarity. In the absence of strong interactions, these studies with PPE help define the role of H bonding and especially the "snug fit", illustrated in Figure 3, which demonstrates the uniqueness of such ligand–receptor interactions. Such information, while essential for receptor modeling studies, should not be taken as being intuitively obvious. This is borne out both by the backwards binding of ligands to PPE[39–41] and by the variation in ligand binding of two heterocyclic inhibitors, an isocoumarin[42] and a benzoxazinone.[43] While the variety of receptor binding modes of heterocyclics remains a puzzle requiring additional crystallographic studies, the binding of derivatized peptide substrates and inhibitors is reasonably well understood; together with the relatively rigid "lock and key" mode of binding exhibited by the serine proteases, molecular modeling is now better equipped to propose novel peptide-like inhibitors.

Based on the reported binding geometry, we conclude that targeted synthesis in this region could provide improved interactions, especially to take advantage of S1′–S3′ interactions provided by Phe-41 (HLE) vs Thr-41 (PPE). Based upon structural homology, similar interactions can be sought at sites further removed in the S′ region. A strong structural homology of the two elastases, HLE and PPE, has been demonstrated. This structural homology is largely limited to the extended binding or receptor site region. Likewise, the structures of peptidic ligands to the two elastases exhibit strong structural homology. Thus, further binding studies of PPE complexes will continue to provide a rich source of information about ligand–receptor interactions, especially for the experimentally less tractable HLE system; molecular modeling of derivatized peptide ligands is thus on firm ground and may be expected to continue to yield fruitful results in the search for useful compounds to treat degenerative diseases like pulmonary emphysema.

(38) Wei, A.-Z.; Mayr, I.; Bode, W. *FEBS Lett.* **1988**, *234*, 367–373.

(39) Hughes, D. L.; Sieker, L. C.; Beith, J.; Dimicoli, J. L. *J. Mol. Biol.* **1982**, *162*, 645–658.

(40) Meyer, E. F.; Radhakrishnan, R.; Cole, G. M.; Presta, L. G. *J. Mol. Biol.* **1986**, *189*, 533–539.

(41) Clore, M. G.; Gronenborn, A.; Carlson, G.; Meyer, E. F. *J. Mol. Biol.* **1986**, *190*, 259–267.

(42) Meyer, E. F.; Presta, L. G.; Radhakrishnan, R. *J. Am. Chem. Soc.* **1985**, *107*, 4091–4093.

(43) Radhakrishnan, R.; Presta, L. G.; Meyer, E. F.; Jr.; Wildonger, R. Crystal Structures of the Complex of Porcine Pancreatic Elastase with Two Valine-Derived Benzoxazinone Inhibitors. *J. Mol. Biol.* **1987**, *198*, 417–424.

Experimental Section

Synthesis. The key step in the preparation of the α,α-difluoro-β-keto amide is the Reformatsky reaction of ethyl bromodifluoroacetate and a protected peptide aldehyde.[44] This reaction gives **1d**, predominantly as a single diastereomer (*S,R*). The relative stereochemistry of the product is presumed to be threo by analogy with the previously reported difluorostatine analogues.[11,45] After further elaboration of the side chains, oxidation of the penultimate alcohol is carried out by the Dess-Martin periodinane oxidation in CH_2Cl_2 which proceeds without loss of stereochemistry to give **1g** as a single diasteromer[46] (Scheme I).

General Methods. Analytical samples were homogeneous by TLC and HPLC and afforded spectroscopic results consistent with the assigned structures. Proton NMR spectra were obtained by using either a Bruker WM-250 or an IBM NR-80 spectrometer. Chemical shifts are reported in parts per million relative to Me_4Si as an internal standard. Mass spectra (MS) were recorded on a Kratos MS-80 instrument operating in either the electron impact (EI) or chemical ionization (CI) mode as indicated. Elemental analyses for carbon, hydrogen, and nitrogen were determined by the ICIA Analytical Department on a Perkin-Elmer 241 elemental analyzer and are within ±0.4% of theory for the given formula. Analytical high-pressure chromatography was conducted on a Zorbax ODS analytical column with a Beckman Liquid Chromatography 340 instrument. Analytical thin-layer chromatography (TLC) was conducted on prelayered silica gel GHLF plates (Analtech, Newark, DE). Visualization of the plates were accomplished by using UV light and/or phosphomolybdic acid–sulfuric acid charring. Flash chromatography was conducted on Kieselgel 60, 230–400 mesh (E. Merck, Darmstadt, West Germany). Solvents were either reagent or HPLC grade. Solvent mixtures are expressed as volume:volume ratios. Solutions were evaporated under reduced pressure with a rotary evaporator. Starting materials were commercially available and were used as received.

(*S*)-*N*-acetyl-L-alanyl-*N*-[3,3-difluoro-1-(1-methylethyl)-2,4-dioxo-4-[(2-phenylethyl)amino]butyl]-L-prolinamide (1) was prepared for crystallographic analysis of its complex with porcine pancreatic elastase. Kinetic analysis of **1** has shown that it is a potent competitive inhibitor of PPE with a $K_i = 5.4 \times 10^{-6}$ M (pH 5.5) when analyzed versus the synthetic substrate MEO-SUC-Ala-Ala-Pro-Val-pNA.[1,12]

[*S*-(*R,*R**)]-2-[[[1-(Hydroxymethyl)-2-methylpropyl]amino]carbonyl]-1-pyrrolidinecarboxylic Acid Phenylmethyl Ester (1a).** A solution of Cbz-proline (180.0 g) in dry tetrahydrofuran (3.0 L) was cooled to −20 °C under N_2 and *N*-methylmorpholine (79.4 mL), followed by isobutyl chloroformate (98.6 g), was added. The reaction mixture was stirred at −20 °C for 15 min and then cooled to −40 °C and a solution of L-valinol (74.5 g) in tetrahydrofuran (500 mL) was added dropwise. The reaction mixture was allowed to warm to room temperature overnight. The reaction mixture was filtered, and the filtrate was diluted with ethyl acetate (1 L) and then washed successively with 1 N HCl (750 mL), $NaHCO_3$ (750 mL), and brine (250 mL). The organic layer was dried over Na_2SO_4, filtered, and concentrated to give **1**: 227.9 g, 94.4%; MS, *m/z* 335 $(M + 1)^+$; ^1H NMR (250 MHz, DMSO-d_6) δ 0.78 (m, 6 H), 1.8 (m, 4 H), 2.08 (m, 1 H), 3.4 (m, 5 H), 4.2 (m, 1 H), 4.50 (m, 1 H, OH), 5.0 (m, 2 H), 7.36 + 7.30 (s, s, 5 H), 7.52 (m, 1 H); Anal. ($C_{18}H_{26}N_2O_4$) C, H, N,; $[\alpha]^{23}_D$ −110.0°.

[*S*-(*R,*R**)]-2-[[(1-Formyl-2-methylpropyl]amino]carbonyl]-1-pyrrolidinecarboxylic Acid Phenylmethyl Ester (1b).** A solution of oxalyl chloride (173.1 g) in dry CH_2Cl_2 (1.5 L) was cooled to −60 °C and a solution of DMSO (213.2 g) in CH_2Cl_2 (300 mL) was added dropwise, maintaining the reaction mixture temperature at −45 °C. The reaction mixture was allowed to warm to −30 °C and a solution of **1** (227.8 g) in CH_2Cl_2 (700 mL) was added dropwise. The reaction mixture was stirred at −25 °C for 1 h and cooled to −40 °C, and a solution of diisopropylethylamine (475 mL) was added dropwise while maintaining the reaction mixture at −40 °C. The reaction was warmed to room temperature and then washed with 1 N HCl (2×; 2 L, 1 L) and brine (1 L). The organic layer was dried over Na_2SO_4 and filtered and the filtrate concentrated under vacuum to give **2**: 226 g, 100%; TLC, silica gel, R_f = 0.6, $CHCl_3$–MeOH (95:5); ^1H NMR (250 MHz, DMSO-d_6) δ 0.83 (m, 6 H), 1.8 (m, 3 H), 2.15 (m, 2 H), 3.49 (m, 2 H), 4.08 (dd, *J* = 7.5 Hz, 1 H), 4.37 (m, 1 H), 5.05 (m, 2 H), 7.32 + 7.36 (s, s, 5 H), 8.24 (m, 1 H), 9.39, 9.45 (s, s, 1 H); Anal. ($C_{18}H_{24}N_2O_4 \cdot 0.5H_2O$) C, H, N.

2-[[[3,3-Difluoro-2-hydroxy-1-(1-methylethyl)-4-(ethoxy-4-oxobutyl]-amino]carbonyl]-1-pyrrolidinecarboxylic Acid Phenylmethyl Ester (1c). A suspension of Zn (3.5 g) and **2** (17.5 g) in dry tetrahydrofuran (300 mL) was heated to reflux under N_2. Ethyl bromodifluoroacetate (11.0 g) was added, and the reaction was refluxed for 1 h. An additional portion of ethyl bromodifluoroacetate (10.98 g) was added, and the reaction was refluxed for 3 h. The reaction mixture was cooled to room temperature and ethyl acetate (800 mL) was added. The mixture was washed with 1 M $KHSO_4$ and brine and dried over $MgSO_4$. The organic layer was filtered and concentrated under vacuum to give the crude product. Flash chromatography of the crude residue on silica gel with ethyl acetate–petroleum ether (1:1) gave **3**: 9.72 g, 39.2%; MS (DCI), *m/z* 456[5] $(M + H)^+$; ^1H NMR (250 MHz, DMSO-d_6) δ 0.66–1.0 (m, 3 H), 1.25 (t, *J* = 7.5 Hz, 3 H), 1.72 (m, 4 H), 2.07 (m, 1 H), 3.39 (m, 2 H), 3.8 (t, *J* = 7.0 Hz, 1 H), 4.1 (m, 1 H), 4.28 (q, *J* = 7.0 Hz, 2 H), 4.3 (m, 2 H), 5.0 (m, 2 H), 6.22 (m, 1 H), 7.3 + 7.35 (s, s, 5 H), 7.57 (m, 1 H); Anal. ($C_{25}H_{34}F_2N_4O_5 \cdot 0.5H_2O$) C, H, N.

2-[[[3,3-Difluoro-2-hydroxy-1-(1-methylethyl)-4-oxo-4-[(2-phenylethyl)amino]butyl]amino]carbonyl]-1-pyrrolidinecarboxylic Acid Phenylmethyl Ester (1d). A solution of **3** (4.0 g) and 2-phenylethylamine (2.13 g) in ethanol (100 mL) was stirred at reflux for 4 h, cooled to room temperature and stirred for an additional 48 h under N_2. The solvent was removed under vacuum, the residue was dissolved in ethyl acetate (100 mL), and the solution was washed with 1 N HCl and brine. The organic layer was dried over $MgSO_4$ and filtered and the solvent removed under vacuum. Flash chromatography of the resulting residue on silica gel with chloroform–methanol (97:3) gave **4**: 4.01, 86.2%; TLC, R_f = 0.60, $CHCl_3$–CH_3OH (95:5); MS (CI), *m/z* 532 $(M + 1)^+$; ^1H NMR (250 MHz, DMSO-d_6) δ 0.78 (m, 6 H), 1.80 (m, 4 H), 2.05 (m, 1 H), 2.77 (t, *J* = 7.0 Hz, 2 H), 3.3 (m, 2 H), 3.76 (m, 1 H), 4.25 (m, 2 H), 5.0 (m, 2 H), 6.02 (m, 1 H), 7.28 (m, 5 H), 7.50 (t, *J* = 10.0 Hz, 1 H), 8.63 (br s, 1 H).

***N*-[3,3-Difluoro-2-hydroxy-1-(1-methylethyl)-4-oxo-4-[(2-phenylethyl)amino]butyl]-2-pyrrolidinecarboxamide (1e).** A mixture of **4** (3.8 g) and 10% palladium on carbon (0.3 g) in ethanol (150 mL) was placed under 1 atm H_2 for 2 h. The mixture was filtered through Celite and the filtrate was concentrated under vacuum to give **5**: 2.46 g, 86.6%; MS (CI), 398 $(M + 1)^+$; ^1H NMR (250 MHz, DMSO-d_6) δ 0.79 (d, *J* = 6.7 Hz, 3 H), 0.85 (d, *J* = 6.6 Hz, 3 H), 1.73 (m, 4 H), 1.94 (m, 1 H), 2.7 (m, 4 H), 3.57 (dd, *J* = 9 Hz, 1 H), 3.73 (m, 1 H), 4.18 (m, 1 H), 6.24 (d, *J* = 7.0 Hz, 1 H), 7.20 (m, 5 H), 8.02 (d, *J* = 10.0 Hz, 1 H), 8.72 (m, 1 H); Anal. ($C_{20}H_{29}F_2N_3O_3 \cdot 1.0H_2O$) C, H, N.

***N*-Acetyl-L-alanyl-*N*-[3,3-difluoro-2-hydroxy-1-(1-methylethyl)-4-oxo-4-[(2-phenylethyl)amino]butyl]-L-prolinamide (1f).** 1-Ethyl-[3-(3-dimethylamino)propyl]carbodiimide hydrochloride (1.01 g) was added to a solution of 1-hydroxybenzotriazole hydrate (0.97 g), **5** (1.85 g), and *N*-acetylalanine (0.61 g) in dry CH_2Cl_2 (20 mL). The reaction mixture was stirred at room temperature for 24 h. The solvent was removed under vacuum, and ethyl acetate (50 mL) was added to the resulting residue. The mixture was filtered, and the filtrate was concentrated under vacuum. Flash chromatography of the resulting residue on silica gel with chloroform–methanol (97:3) gave **6**: 0.98 g, 41%; TLC, R_f = 0.51, $CHCl_3$–CH_3OH (90:10); MS (DCI), *m/z* 511 $(M + 1)^+$; ^1H NMR (250 MHz, DMSO-d_6) δ 0.82 (d, *J* = 6.8 Hz, 3 H), 0.85 (d, *J* = 6.5 Hz, 3 H), 1.165 (d, *J* = 6.9 Hz, 3 H), 1.8 (s, 3 H), 1.85 (m, 5 H), 2.77 (t, *J* = 7.8 Hz, 2 H), 3.34 (m, 2 H), 3.56 (m, 2 H), 3.73 (t, *J* = 7.5 Hz, 1 H), 4.2 (m, 2 H), 4.4 (s, 1 H), 4.51 (t, *J* = 7.5 Hz, 1 H), 6.0 (d, *J* = 7.5 Hz, 1 H), 7.23 (m, 5 H), 7.42 (d, *J* = 9.6 Hz, 1 H), 8.15 (d, *J* = 7.5 Hz, 1 H), 8.6 (m, 1 H).

(*S*)-*N*-Acetyl-L-alanyl-*N*-[3,3-difluoro-1-(1-methylethyl)-2,4-dioxo-4-[(2-phenylethyl)amino]butyl]-L-prolinamide (1g). Trifluoroacetic acid (0.69 mL) was added to a stirred solution of **6** (0.95 g) and Dess-Martin periodinane (3.74 g) in CH_2Cl_2 (25 mL). The mixture was stirred overnight at room temperature under N_2. Ethyl acetate (100 mL) was added, the mixture was washed successively with saturated NaS_2O_3, saturated $NaHCO_3$, and brine, the organic layer was dried over $MgSO_4$ and filtered, and the solvent was removed under vacuum. Flash chromatography of the resulting residue on silica gel with $CHCl_3$–CH_3OH (97:30) gave **7**: 0.433 g, 48%; HPLC, t_R = 8.37 min, flow rate = 1.0 mL/min, CH_3CN–H_2O (40:60), ZORBAX ODS analytical column; MS (DCI), *m/z* = 509 $(M + 1)^+$; ^1H NMR (250 MHz, DMSO-d_6) δ 0.8 (d, *J* = 6.8 Hz, 3 H), 0.88 (d, *J* = 6.8 Hz, 3 H), 1.4 (d, *J* = 6.8 Hz, 3 H), 1.8 (s, 3 H), 1.83 (m, 4 H), 2.25 (m, 1 H), 2.76 (t, *J* = 7.7 Hz, 2 H), 3.34 (m, 2 H), 3.58 (m, 2 H), 4.49 (m, 2 H), 4.75 (m, 1 H), 7.23 (m, 5 H), 8.13 (d, *J* = 7.5 Hz, 1 H), 8.25 (d, *J* = 8.2 Hz, 1 H), 9.2 (t, *J* = 7.5 Hz, 1 H); $[\alpha]^{23}_D$ = −68.0°; Anal. ($C_{25}H_{34}F_2N_4O_5 \cdot 0.5H_2O$) C, H, N.

Crystallographic Data Collection. Crystals of PPE were grown from commercially available elastase (Serva 20909) without further purification. The crystals were grown from a 2.0% (w/v) solution of PPE in 0.1 M sodium phosphate, 0.1 M sodium sulfate (pH 5.0) by vapor diffusion. Crystals suitable for X-ray diffraction were placed into a dialysis button, and an excess of the inhibitor (ca. 1 mg/mL) was dissolved in the same buffer and allowed to diffuse gently into the crystal. After 24 h of soaking, a crystal [space group $P2_12_12_1$; cell dimensions *a* = 51.24 (17), *b* = 58.17 (10), *c* = 75.54 (26) Å] of approximate dimensions 0.5 mm

(44) Hallinan, E.; Fried, J. *Tetrahedron Lett.* **1984**, *25*, 230.
(45) Thaisrivongs, S.; Pals, D. T.; Kati, W. M.; Turner, S. R.; Thomasco, L. M. *J. Med. Chem.* **1985**, *28*, 1555.
(46) Dess, D. B.; Martin, J. C. *J. Org. Chem.* **1983**, *48*, 4156.

× 0.5 mm × 0.9 mm was mounted along the elongated *b* axis in a thin-walled glass capillary tube with a small amount of mother liquor.

Diffraction data to 1.78 Å resolution were collected at 19 °C on a modified Nonius precession camera using the rotation mode, flat-film cassette, with a crystal-to-film distance of 48.4 mm. A Rigaku Denki rotating-anode generator operating at 3.6 kW and a monochromatized (pyrolytic graphite) beam were used with a 0.5-mm collimator. By use of Kodak DEF-2 film, data were collected over 3° rotation intervals, the usual rate being 3°/3 h.

The intensity of the reflections was measured by means of an Optronics rotating-drum densitometer and evaluated by program FILME.[47] After completion of the 90° scan about the *b* axis, the crystal was mounted about the *c* axis and an additional 21° was scanned.

Data processing was performed by the PROTEIN program system of Steigemann.[17] Separate films were scaled and multiple measurements of the same reflection including those related by symmetry were merged. The internal consistency checking feature of the PROTEIN program was used to delete reflections exhibiting gross discrepancies. This method corrects for slight crystal decay. Based upon similar studies,[14] radiation damage is typically less than 5% over 7 days. Here, 5 days was required for complete data collection; no correction for crystal decay nor absorption was made. R_{merge} measures the agreement of intensity measurements from each source with mean values obtained from several sources and is defined as $\sum|I_i - \langle I\rangle|/\sum I_i$, where I_i is the intensity value of individual measurements and $\langle I\rangle$ the corresponding mean values, the summation being over all measurements common to two or more films. R_{merge} values ranged from 0.068 to 0.123 with a mean R_{merge} value of 0.087. R_{symm} (defined as $\sum|I_i - \langle I\rangle|/\sum I_i$, where $\langle I\rangle$ is the average intensity and I_i the intensity of individual measurements with symmetrical correspondence) was in the range of 0.043-0.078. Of 36 367 reflections above FILME's 1σ significance level, 16 151 unique reflections, comprising 71% of the possible reflections to 1.78 Å resolution, were obtained. As a separate evaluation of the effective resolution of the data, Sparrow's resolution criterion was employed,[23] giving 1.98 Å for this data set. Both reflection data and coordinates are deposited with Protein Data Bank.[48,49]

Acknowledgment. We wish to acknowledge the assistance of Anne Strimpler with biochemical measurements. Diffraction facilities were provided, thanks to the hospitality of Prof. Robert Huber. Computational facilities were provided by Dr. John Dinkel, Provost for Computing, Teaxs A&M University.

Registry No. 1a, 95924-70-2; **1b**, 109522-66-9; **1c**, 109522-75-0; **1d**, 109522-76-1; **1f**, 119720-82-0; **1g**, 119720-81-9; PPE, 9004-06-2; $BrCF_2COOEt$, 667-27-6; $PhCH_2CH_2NH_2$, 64-04-0; Ac-L-Ala, 97-69-8; Cbz-proline, 1148-11-4; L-valinol, 2026-48-4.

(47) Schwager, P.; Bartels, K.; Jones, T. A. *J. Appl. Crystallogr.* **1975**, *8*, 275-280, with improvements by William S. Bennett.

(48) Bernstein, F. C.; Koetzle, T. F.; Williams, G. J. B.; Meyer, E. F., Brice, M. D.; Rodgers, J. R., Kennard, O.; Shimanouchi, T.; Tasumi, J. *J. Mol. Biol.* **1977**, *112*, 535-542; *Eur. J. Biochem.* **1977**, *80*, 319-324.

(49) Diffraction data and coordinates have been deposited in the Protein Data Bank[48] and have been assigned the access codes R4ESTSF and 4EST.

Structural Requirements for Catalysis by Chorismate Mutase

John L. Pawlak, Robert E. Padykula, John D. Kronis, Robert A. Aleksejczyk, and Glenn A. Berchtold*

Contribution from the Department of Chemistry, Massachusetts Institute of Technology, Cambridge, Massachusetts 02139. *Received June 23, 1988*

Abstract: The structural requirements for mutase-catalyzed Claisen rearrangement by chorismate mutase-prephenate dehydrogenase from *Escherichia coli* have been established. The chorismate analogue lacking the carboxyl group at C_1 (**5**) was not a substrate for chorismate mutase. The methyl ether of chorismate [(±)-**6**] was a good substrate for chorismate mutase ($k_{cat}/k_{uncat} = 2.0 \times 10^4$). The half-lives for Claisen rearrangement and aromatization of 4-deshydroxychorismate (**19**) in D_2O at 30 °C, pD 7.2, were 3.5 and 8 min, respectively. In the presence of large amounts of enzyme, it was demonstrated that the Claisen rearrangement of enantiomerically pure **19** was accelerated at least 100-fold by chorismate mutase. Data available from other studies have demonstrated that ester **3** is not a substrate for chorismate mutase, and the k_{cat}/k_{uncat} for dihydrochorismate analogue **4** is similar to that for chorismate. These results establish that the only functional groups required on the allyl vinyl ether moiety of chorismate for mutase-catalyzed rearrangement are the two carboxylate groups.

Chorismate (**1**) is the branch-point intermediate in the biosynthesis of aromatic amino acids and growth factors in bacteria, fungi, and higher plants.[1] The first step in the biosynthesis of phenylalanine and tyrosine from **1**, the intramolecular rearrangement to prephenate (**2**), is catalyzed by the enzyme chorismate mutase (Scheme I). The uncatalyzed rearrangement of **1** to **2** occurs readily in aqueous solution with a half-life of 15.7 h at 30 °C, pH 7.5.[2] Chorismate mutase accelerates the rearrangement by a factor of 2×10^6 at 37 °C, pH 7.5.[2] Both the uncatalyzed[3] and the enzyme-catalyzed[4,5] reactions proceed through a chairlike transition state.

Scheme I

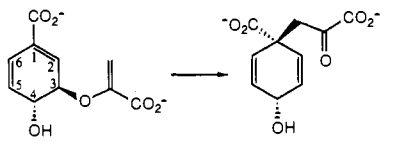

1 **2**

Chart I

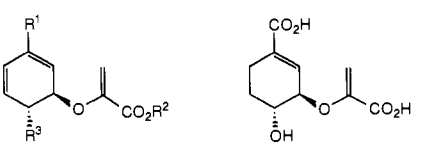

3, R^1=CO_2H, R^2=Me, R^3=OH
5, R^1= R^2=H, R^3=OH
6, R^1=CO_2H, R^2=H, R^3=OMe
7, R^1=CO_2H, R^2=R^3=H

4

The chorismate mutase catalyzed Claisen rearrangement of **1** to **2** appears to be the only established example of an enzyme-catalyzed pericyclic reaction in primary metabolism.[6] This unique

(1) For reviews see: (a) Weiss, U.; Edwards, J. M. *The Biosynthesis of Aromatic Compounds*; Wiley: New York, 1980. (b) Haslam, E. *The Shikimate Pathway*; Halstead Press, Wiley: New York, 1974. (c) Ganem, B. *Tetrahedron* **1978**, *34*, 3353-3383.

(2) Andrews, P. R.; Smith, G. D.; Young, I. G. *Biochemistry* **1973**, *12*, 3492-3498.

(3) Copley, S. D.; Knowles, J. R. *J. Am. Chem. Soc.* **1985**, *107*, 5306-5308.

(4) Sogo, S. G.; Widlanski, T. S.; Hoare, J. H.; Grimshaw, C. E.; Berchtold, G. A.; Knowles, J. R. *J. Am. Chem. Soc.* **1984**, *106*, 2701-2703.

(5) Asano, Y.; Lee, J. J.; Shieh, T. L.; Spreafico, F.; Kowal, C.; Floss, H. G. *J. Am. Chem. Soc.* **1985**, *107*, 4314-4320.

0002-7863/89/1511-3374$01.50/0